

## ORIGINAL ARTICLE

# Synthesis of Chitosan Collagen Nanoparticles from Iraqi Catfish (Siluriformes) Skin and Evaluation of their Antibacterial Activity

Dooa M. Jebur\*, Shurook M.K. Saadedin

Institute of genetic engineering and Biotechnology for Higher Studies, University of Baghdad, Iraq

## ABSTRACT

### Key words:

Collagen, Nanocollagen, Chitosan, FTIR, XRD

### \*Corresponding Author:

Dooa Mohammed Jebur,  
Institute of Genetic  
Engineering and Biotechnology  
for Postgraduate Studies,  
University of Baghdad/ Iraq  
Tel.: 009647716888349  
[mdidy00@gmail.com](mailto:mdidy00@gmail.com)  
ORCID: 0009-0008-1812-4219

**Background:** Chitosan-collagen nanoparticles have emerged as promising materials for biomedical applications due to their excellent biocompatibility, biodegradability, and antimicrobial properties. The synthesis of nanocollagen from Iraqi catfish (*Siluriformes*) skin using chitosan and sodium tripolyphosphate (STPP) as crosslinking agents represents an innovative approach to creating biocompatible nanoparticles. The study utilizes various analytical techniques such as FTIR, UV-Vis, XRD, and SEM to characterize and understand the properties of nanoparticles. **Objective:** This study aimed to evaluate the efficacy of nano-collagen in managing infections caused by multidrug-resistant bacteria such as *Staphylococcus aureus* and *Pseudomonas aeruginosa*. **Methodology:** Bacterial isolates were collected from patients with wound infections at the Al-Zahrawi Hospital in Maysan. Identification was confirmed using selective media (MacConkey agar and mannitol salt agar) and standard microbiological tests, including Gram staining and biochemical assays. The Vitek-2 system was used for precise bacterial identification. **Results:** Minimum inhibitory concentration (MIC) tests demonstrated that nano-collagen doubled the antibacterial efficacy of collagen extract. The MIC was 47.5 µg/mL (nano-collagen) vs. 95 µg/mL (collagen extract). against *S. aureus* the MIC was 95 µg/mL (nano-collagen) vs. 380 µg/mL (collagen extract). **Conclusion:** These findings suggest that nanocollagen is a promising biomaterial for regenerative medicine and advanced wound care.

## INTRODUCTION

Skin infections resulting from bacterial contamination represent a significant challenge for the medical community worldwide. Among the most notorious pathogens associated with these infections are *Staphylococcus aureus* and *Pseudomonas aeruginosa*, both of which exhibit alarming resistance to conventional therapies<sup>1</sup>. This growing antimicrobial resistance highlights the urgent need for innovative and effective solutions to enhance wound healing and combat bacterial infections<sup>2</sup>. In light of the increasing reliance on natural resources and advanced technologies, marine-derived collagen has emerged as a promising material that combines biological efficacy with environmental sustainability<sup>3</sup>. Several recent studies have emphasized the importance of marine collagen, particularly from fish skin, for its ability to promote tissue regeneration and reduce inflammation, making it a valuable resource for wound healing. Collagen is a fundamental protein comprising 25-35% of the total protein in the human body, with type I collagen constituting up to 70% of skin tissue<sup>4</sup>. It is a triple-helical protein composed of multiple peptide chains that provide structural integrity and functionality to tissues, with over 29 known types, collagen plays a pivotal role in tissue support and stabilization<sup>5</sup>.

The skin of Iraqi catfish (*Siluriformes*) serves as a sustainable and unconventional source of high-quality collagen, distinguished by its biodegradability and ease of absorption. Advances in nanotechnology have enabled the transformation of collagen into nanocollagen, significantly enhancing its mechanical, biochemical, and biological properties<sup>6</sup>. Nanotechnology is characterized by any technical progress involving nanoscale materials that can be utilized in everyday life<sup>7</sup>. This entails the manipulation of matter possessing at least one dimension, ranging from approximately 1 to 100 nm in size. This technique encompasses the synthesis of nanomaterials applicable to many physical, chemical, and biological systems, facilitating integration at both microscopic and macroscopic scales<sup>8</sup>. Nano collagen is a standard collagen that is reduced to the nanometer scale<sup>9</sup>. This 3D biomaterial is optimal because of its nanoscale technology ranging from 1 to 100 nm, which offers a high surface-area-to-volume ratio, facilitating efficient penetration into wound sites and effective interaction. When combined with chitosan, a natural polysaccharide with antimicrobial properties, nanocollagen offers unique advantages<sup>7</sup>. The current study aimed to manufacture nano-collagen using chitosan, study its physical and chemical properties, and evaluate the effect of nano-collagen against *Staphylococcus aureus* and *Pseudomonas aeruginosa*.

## METHODOLOGY

### Sample collection

Parts of catfish were collected in an ice box from a local market in Myssan and stored at  $-18^{\circ}\text{C}$ . The skin of 12 catfish was used in this experiment. Commercial collagen from the scales of fish type II and collagen I was purchased from Baoding Faithful Industry Co., Ltd. (Which were used as reference control). All chemicals used in this study were of analytical grade unless otherwise stated.

### Collagen Extraction

The catfish skin underwent a series of preparatory and chemical treatments to isolate collagen. Initially, the skin was cleaned and washed to remove surface impurities. Non-collagenous proteins were extracted by soaking the skin in 0.1 M NaOH at a ratio of 30:1 (v/w) for 24 hours, with the solution replaced every 8 hours. Subsequently, defatting was performed by treating the skin with 10% butyl alcohol at a 30:1 ratio (v/w) for 24 hours under continuous agitation. For collagen solubilization, the treated skin was soaked in 0.5 M acetic acid, followed by filtration to obtain a collagen-rich solution. Collagen was then precipitated by adding 2.6 M NaCl in 0.05 M Tris-HCl buffer (pH 7.0). The resulting precipitate was centrifuged at 10,000 rpm under cooled conditions, dialyzed against 0.1 M acetic acid and distilled water, and finally lyophilized for long-term preservation<sup>10</sup>.

### Nanocollagen Preparation

Nanoparticles were synthesized using chitosan and sodium tripolyphosphate (STPP) following ionic gelation. Chitosan was dissolved in 1% acetic acid and stirred for activation. Collagen was dissolved in DMSO and combined with chitosan in a 1:1 molar ratio. Crosslinking was induced by adding STPP (1:2.5 ratio, w/w) and stirring at room temperature for 6 h. The nanoparticles were collected via filtration, washed with ethanol and deionized water, and freeze-dried for further analysis<sup>11</sup>.

### Characterization of nanocollagen

The UV-Vis absorption spectra of ASC and PSC were measured using a SELECTA SPAIN spectrophotometer within the wavelength range of 200 to 300 nm<sup>12,13</sup>. Additionally, Fourier-transform infrared spectroscopy (FTIR) analysis was conducted using potassium bromide (KBr) pellets. These pellets were prepared by mixing 2 mg of dried collagen with 200 mg of KBr, which were then compressed into discs. The FTIR measurements were carried out using a SHIMADZU (Japan) instrument, covering a spectral range of 400 to 4000  $\text{cm}^{-1}$ <sup>14</sup>. A thin film of uniformly suspended water containing each type of nanoparticle was prepared on a glass slide and dried. X-ray diffraction (XRD) patterns were recorded using an X-ray diffractometer in  $2\theta/\theta$  scanning mode (operational

voltage 40 kV and current 30 mA, Cu K(a) radiation  $\lambda = 1.540$ )<sup>15</sup>.

Data were recorded in the  $2\theta$  range of  $10^{\circ}$ – $80^{\circ}$  with a step of  $0.0200^{\circ}$ . The results obtained from the XRD pattern were interpreted using the standard reference of the Joint Committee on Powder Diffraction Standards (JCPDS card number 04-0783) for the characterization of C-CsNPs. The particle sizes of the prepared samples were determined using the Debye–Scherrer equation<sup>12</sup> as follows :

$$D = \beta \cdot \cos \theta / k \cdot \lambda \quad \text{is} \quad \lambda \quad \text{Where } D \text{ is the crystal size,} \\ \dots\dots\dots (2)$$

The wavelength of the X-rays,  $\theta$ , is the diffraction angle (Bragg angle) in radians, and  $\beta$  is the full width at half maximum (FWHM) of the peak in radians. The measurements were performed at Al-Khora Company in Baghdad. The morphological properties of the membranes, such as surface permeability, roughness, and texture were examined. Structural analysis of the extracted collagen was performed using scanning electron microscopy (SEM). The sample was coated with gold using an auto fine ion coater (JEOL JFC-1600), and the surface morphology of the nanoparticles was visualized by **Atomic Force Microscope** Contact mode under normal atmospheric conditions. Samples of nanoparticle solution, drops on a glass slide ( $1 \times 2$ ) cm, were dried and dispersed on the Atomic Force Microscopy (AFM) sample stage. AFM analysis was performed at CAC Company in Baghdad.

### Isolation and identification of bacterial isolates

In this study, ten previously characterized bacterial isolates, comprising *Pseudomonas aeruginosa* and *Staphylococcus aureus*, were obtained from AL-Zahrawe Hospital in Missan during September 2023. These isolates were collected from patients presenting with various clinical conditions, including dermatitis, wound infections, burns, and other skin-related infections. The isolation process employed standard bacteriological methods, utilizing selective culture media such as MacConkey agar for *P. aeruginosa* and mannitol salt agar for *S. aureus*. Subsequent identification and confirmation of all isolates were conducted using the Vitek 2 Compact System, ensuring accurate species-level characterization.

### Determination of Minimum Inhibitory Concentration and Sub-Minimum Inhibitory Concentration (MIC)

The antibacterial activity of Collagen and CSNPs loaded Collagen was evaluated utilizing minimum inhibitory concentration (MIC) and Sub-MIC assays against *p. aeruginosa* and *S. aureus*. The MIC was determined using the 96-well microtiter plate method (MTP) using the resazurin-assisted microdilution technique in Mueller-Hinton broth (MHB), as described by Elshikh et al.<sup>16</sup>. All the bacterial isolates were

subjected to a minimal inhibitory concentration test. MIC was determined after incubation at 37 °C for 24 h on a microtiter plate, and the results were read by an ELISA reader at a wavelength of 630 nm.

### Statistical Analysis

The results were analyzed according to a completely randomized design to study the effect of treatment with the nanocomposite collagen extract and the duration of time in the studied standards, and analysis of variance was used. A complete randomized study to study the effect of treatment with the treatment and the nanocomposite on Skin Wounds The significance of the differences between the means was determined using the Significant Least Revised (LSD) test Differences and T-test to test the differences between the treatment effect of the treatment The length of the treatment period after loading the treatment onto the nanocomposite and using the Spss program.

## RESULTS

### Biosynthesis of Chitosan Collagen nanoparticles (Cs-CNPs)

Chitosan and Collagen adducts were prepared and TPP was added to form CSNPs loaded with collagen, the appearance of a clear color indicated the formation of nanoparticles loaded with the collagen extract.

### Characterization of Chitosan Collagen Nanoparticles UV-Visible spectroscopy

The results shown in Figure (1) indicate the results of UV absorption of collagen, which recorded greatest absorbance value in the collagen was 3.223, at a length 279.00 nm while the lowest absorbance values were 0.024 and 0.092 at wavelengths of 542.00 nm and 430.00 nm, respectively. Figure (2), shown results of UV for CsCNPs, the greatest absorbance value was 1.924 and the lowest absorbance value was 0.006 at wavelengths 261.00 nm and 442.00 nm respectively.

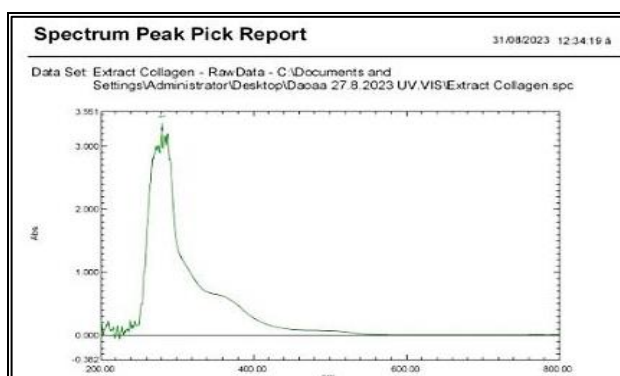


**Fig. 1:** UV-Visible Spectral Analysis of Collagen from Iraqi Catfish Skins.

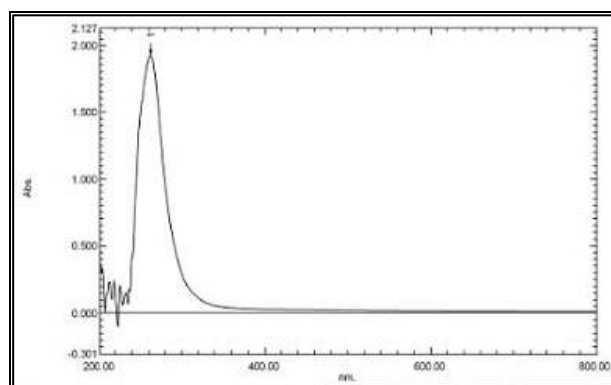


**Fig. 2:** UV-Visible spectral analysis of Chitosan Collagen Nanoparticles from Iraqi catfish skins.

### Fourier transformation infrared spectroscopy (FTIR)

FTIR measurements were performed over a range between 400 through 4000  $\text{cm}^{-1}$ . The present study shows sixteen peak curves of collagen extract and resulted transmittance peaks at 418.55, 563.21, 921.97, 1029.99, 1080.14, 1165.00, 1238.3, 1330.88, 1396.46, 1446.61, 1533.41, 1647.21, 2358.94, 2937.59, 3072.6, 3302.73  $\text{cm}^{-1}$ . Figure (3) The peak 563.21  $\text{cm}^{-1}$  Refers to C-H affinity, the peak 1396.46  $\text{cm}^{-1}$  were denotes group Carbonyl C-O- or C-N group, the peak 1647.21  $\text{cm}^{-1}$  refer to indicates the existence of mono amides and Di amides N-H. The peak at 1080.14  $\text{cm}^{-1}$  indicates the presence of an affinity C-N for amino acids, the peak at 2937.59  $\text{cm}^{-1}$  refer the presence of a C-H group, and the last peak at 3302.73  $\text{cm}^{-1}$  refer the presence of an O-H group<sup>17</sup>. Fourier transform infrared of CSNPs loading collagen refer to ten peaks 511.14, 624.94, 837.11, 1136.07, 1384.89, 1529.55, 1654.92, 2862.36, 2927.94, 3425.58  $\text{cm}^{-1}$ , shown in Figure (4) the 624.94  $\text{cm}^{-1}$  band, is attributed to the vibration of C-C 1384.89  $\text{cm}^{-1}$  band is related to the vibration of C-N, while 1654.92  $\text{cm}^{-1}$  band is related to the stretching vibration of carbonyl (C=O). 2862.36  $\text{cm}^{-1}$  band is related to the stretching vibration of C-H. The last 3425.58  $\text{cm}^{-1}$  indicates the stretching vibrations of the hydroxyl group. The spectra showed a characteristic peak  $\sim 4000 \text{ cm}^{-1}$  which can be attributed to hydroxyl groups participating in inter and intramolecular hydrogen bonding. The FTIR spectra of collagen show several vibrations in the region above 1500  $\text{cm}^{-1}$ , for which the presence of long-chain fatty acids or hydrocarbons cannot provide an explanation. Rather, these features are probably correlated with particular functional groups.

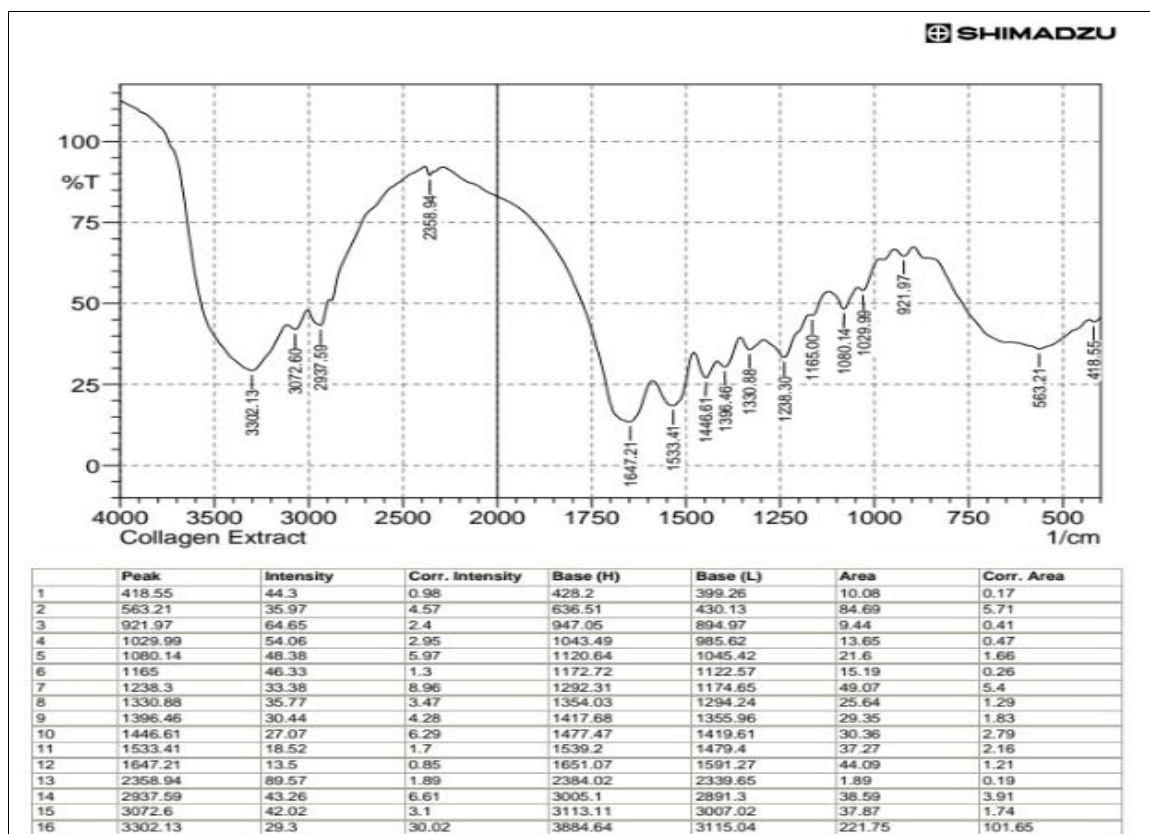


Fig. 3: FTIR Spectra Pattern of collagen from Iraqi catfish skins.

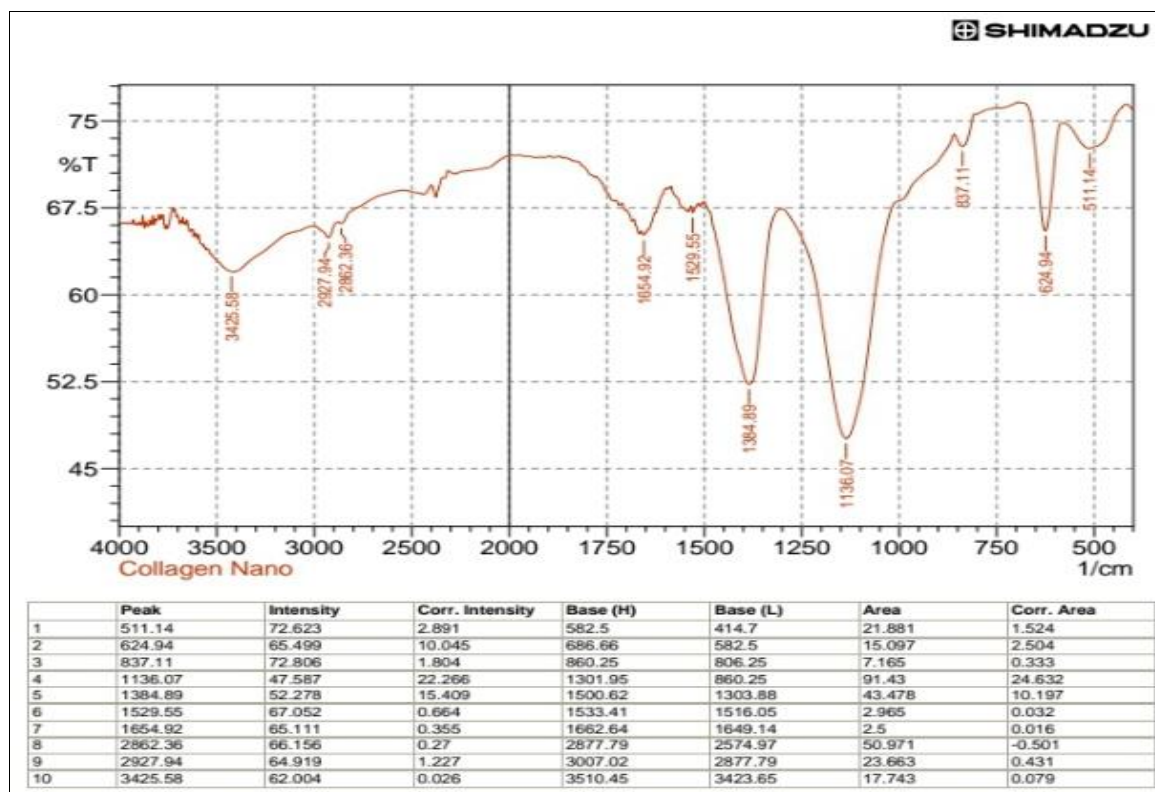
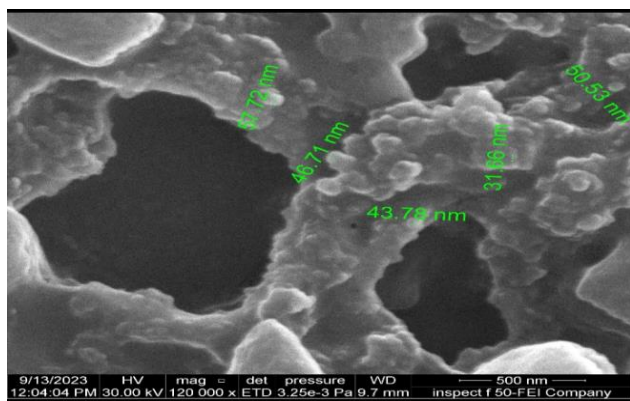


Fig. 4: FTIR Spectra Pattern of chitosan nanoparticul loaded with collagen

### Scanning Electron Microscope (SEM) of Chitosan Collagen Nanoparticles from Iraqi catfish skins

Figure 5 shows the scanning electron microscope (SEM), results where Cs-CNPs have a spherical appearance with a diameter range of 31.66-57.72 nm and have a relatively homogeneous morphology.



**Fig. 5:** SEM image of Chitosan nanoparticles loaded with collagen

### Atomic Force Microscopy (AFM) of Chitosan Collagen Nanoparticles from Iraqi catfish skins

The AFM results shown in Figure (6) indicate the particle size and surface topography of Cs-CNPs, where the particle sizes ranged from 23.14 to 297.7 nm, demonstrating the size distribution of these nanoparticles. The results showed that the collagen-loaded chitosan nanoparticles were fairly homogeneous in shape, with a good size distribution. The statistical measurements provided a quantitative description of the particle size distribution and height, also (Figure 7) shows the 3D image of CsCNPs, revealing a population of homogeneous particles with a regular surface shape.

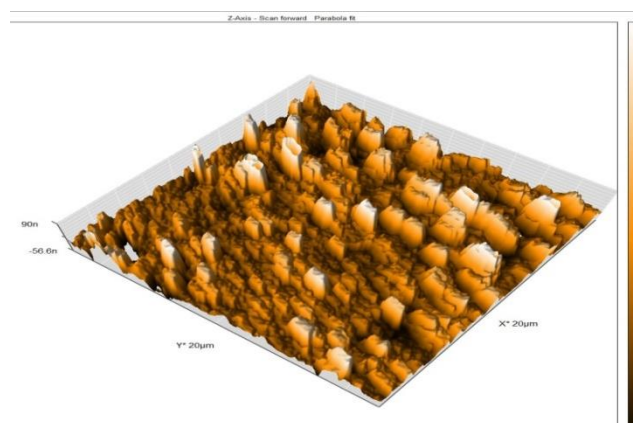


**Figure (6):** 3D image of chitosan–collagen nanoparticles

### Identification of *Pseudomonas. aeruginosa* and *Staphylococcus aureus* using Standard Laboratory Methods.

#### Minimum Inhibitory Concentration Microtiter Plate Method (MTP)

The antimicrobial activities of various formulations were evaluated by Minimum Inhibitory Concentration (MIC) testing. The results demonstrated that The combination of Cs-CNPs and gentamicin exhibited the highest antibacterial potency, with MIC values of 47.5 µg/mL for *P. aeruginosa* and 95 µg/mL for *S. aureus*. In comparison, collagen combined with gentamicin displayed lower antibacterial efficacy, with MIC values of 95 and 380 µg/mL for *P. aeruginosa* and *S. aureus*, respectively. When tested individually, the Cs-CNPs exhibited moderate antibacterial activity, with MIC values of 190 µg/mL for both *P. aeruginosa* and *S. aureus*, as shown in Table (1).

**Table 1:** MIC value against *P. aeruginosa*- *S.aureus*

Isolates	<i>P. aeruginosa</i>	<i>S. aureus</i>	T-test
<b>Chitosan- Collagen Nanoparticles +Gentamicin</b>	47.5	95	17.385**
<b>Collagen+Gentamicin</b>	95	380	26.902**
<b>Chitosan- Collagen Nanoparticles</b>	190	190	15.00NS
<b>T-test</b>	<b>22.074**</b>	<b>35.163**</b>	
	**(P≤0.01).		

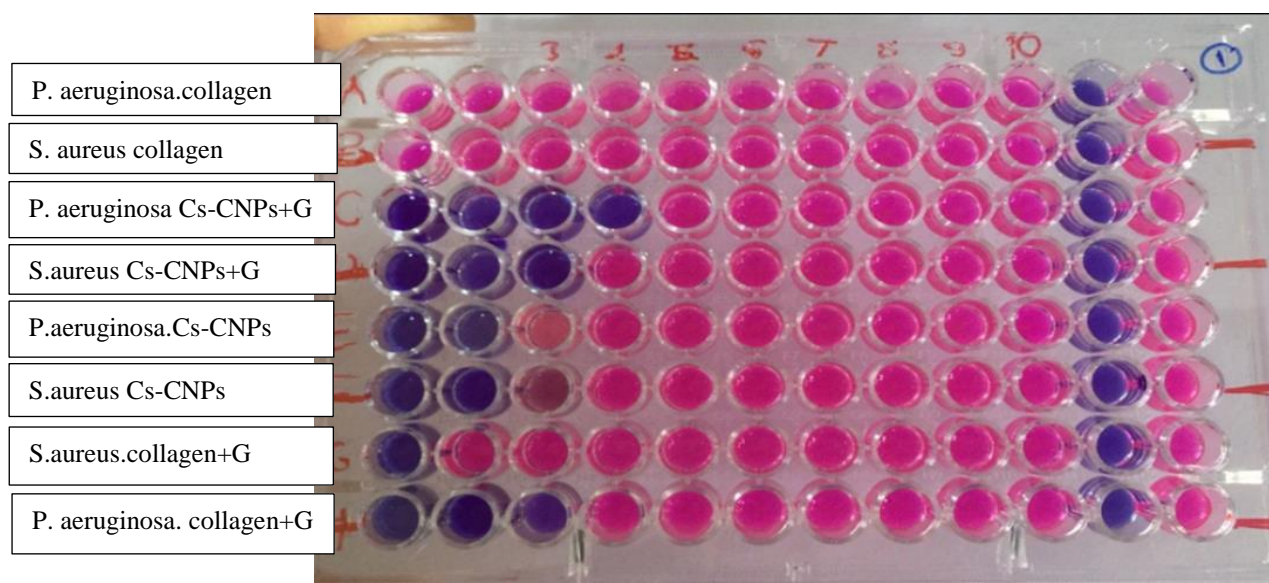


**Fig. 9:** Microtiter plate 96-well of Chitosan- Collagen Nanoparticles on *Pseudomonas aeruginosa* *Staphylococcus aureus* isolates. N.C.: Negative control (only Mueller Hinton broth) P.C.: Positive control (only bacteria *Staphylococcus aureus* or *Pseudomonas aeruginosa*), G: Gentamicin

## DISCUSSION

In the current study, were synthesized Chitosan-Collagen Nanoparticles when chitosan reacts with tripolyphosphate (TPP), the amine groups of chitosan can cross-link with the phosphine groups of TPP to create nanoparticles, which alters the molecular structure of chitosan, resulting in a change in solubility in an acid solution as well as a gel-like solution or a liquid form<sup>18</sup>.

UV-visible spectroscopy is a primary step in confirming the synthesis of Cs-CNPs. The absorbances of collagen and Cs-CNPs were measured. The decrease in absorbance value at wavelength 430-442 nm from 0.092 nm in collagen to 0.006 nm in CSNPs loaded collagen, along with the emergence of new wavelengths with strong absorption. the highest of which was at 261 nm in CSNPs with a value of 1.924 and all loaded with collagen, showing the successful formation of nanomaterial and loading of collagen on the chitosan nanoparticles.

Infrared spectroscopy is very important in providing an idea of the composition of matter, as the infrared spectrum helps to determine the type of chemical groups because each chemical group absorbs a type of radiation of a specific frequency in a specific spectral range, which is expressed in wavelengths to investigate the interactions that occur during the formation of Nano capsulation<sup>19</sup>. Further studies were performed using FTIR. The change in the bonds and the interaction kinetics between the compounds are evidence of the collagen link to CSNPs and the formation of the nanocapsule. Figure (4) indicates the presence of the

transformation process, that is, the compounds were bound and the rest were withdrawn, thus obtaining a highly effective capsule with a low concentration. SEM shown the larger particles may be a result of the unwanted aggregation that occurs throughout the drying process, and agglomeration occurs as soon as the liquid evaporates, resulting in an increased particle concentration. The rise in dissolved ion concentration due to liquid evaporation might diminish the electrostatic repulsive force that promotes agglomeration<sup>20</sup>.

This study evaluated the antibacterial efficacy of chitosan-based nanoparticles (Cs-CNPs) and collagen, both individually and in combination with the antibiotic gentamicin, against two bacterial strains, *Pseudomonas aeruginosa* and *Staphylococcus aureus*. This enhancement is likely attributable to the structural properties of bacterial cell walls, which influence their susceptibility to chitosan-based compounds. Gram-positive bacteria, such as *S. aureus*, with their thick peptidoglycan layer, may be more accessible to the disruptive actions of chitosan nanoparticles, while gram-negative bacteria, such as *P. aeruginosa*, with their outer membrane, may exhibit reduced susceptibility due to additional permeability barriers.

The observed synergistic effects are consistent with previous studies that have explored the combination of chitosan nanoparticles with antibiotics. For instance, Swethavinayagam et al. (2021) reported that ciprofloxacin-conjugated chitosan nanoparticles exhibited enhanced antibacterial activity against *S. aureus* and *E. coli*, with *S. aureus* showing greater susceptibility<sup>21</sup>. This parallels our findings, where *S.*

*aureus* demonstrated a more pronounced response to the Cs-CNPs-gentamicin combination. Similarly, Kadhum and Zaidan (2020) demonstrated that chitosan-alginate nanoparticles loaded with doxycycline exhibited superior antibacterial efficacy against multidrug-resistant (MDR) gram-negative and gram-positive bacteria compared to native doxycycline. These results underscore the potential of chitosan-based nanoparticles to enhance the delivery and efficacy of antibiotics, particularly against resistant strains<sup>22</sup>.

Furthermore, the antibacterial activity of chitosan-collagen nanocomposite films containing metal nanoparticles, as reported in prior research, supports the utility of chitosan-based composites in combating bacterial infections. Notably, *P. aeruginosa* and methicillin-resistant *S. aureus* (MRSA) were found to be highly sensitive to these films, highlighting the broad-spectrum potential of chitosan-based formulations. This is particularly relevant in the context of multidrug-resistant pathogens, where conventional antibiotics often fail to achieve therapeutic efficacy<sup>23</sup>.

Collectively, these studies, including our own, emphasize the promising role of chitosan-based nanoparticles as adjuvants to antibiotics. The enhanced antibacterial activity observed in our study, particularly against *S. aureus*, suggests that the combination of Cs-CNPs with gentamicin could be a viable strategy for overcoming bacterial resistance. However, the differential responses observed between gram-positive and gram-negative bacteria underscore the need for further investigation into the mechanisms underlying these variations.

## CONCLUSION

**Enhanced Antibacterial Activity:** Nano-collagen particles showed a more potent antibacterial effect against antibiotic-resistant bacteria, specifically *Pseudomonas aeruginosa* and *Staphylococcus aureus*, when compared to the extracted collagen. The nanoformulation exhibited a reduced minimum inhibitory concentration, indicating higher antibacterial efficacy. Nanotechnology as a key to medical advances: This study demonstrates powerful applications of nanotechnology in medicine, particularly in enhancing the properties of natural materials for therapeutic purposes. Nano-collagen and chitosan present promising avenues for the development of next-generation of topically applied treatment that address both healing and infection control.

### Declarations

**Availability of data and material** The datasets used and analyzed during the current study are available from the corresponding author on reasonable request.

**Competing interests** The author declare that they have no competing interests

**Funding** No funds were received to fulfil this work.

**Acknowledgements** We are truly grateful to the patients who supplied samples for our study despite their challenging medical conditions. Additionally, we thank the laboratories of the Institute for Genetic Engineering and Biotechnology for Postgraduate Studies, University of Baghdad, for their essential contribution to the practical aspects of this study.

**Author Contribution** The authors were contributed equally in conceptualized the research, collected data, participated in data analysis and write-up, editing and review.

## REFERENCES

1. Edlich R, Winters KL, Britt LD, Long III WB. Bacterial diseases of the skin. *J Long Term Eff Med Implants*. 2005;15(5).
2. Meneghetti KL, do Canto Canabarro M, Otton LM, dos Santos Hain T, Geimba MP, Corção G. Bacterial contamination of human skin allografts and antimicrobial resistance: a skin bank problem. *BMC Microbiol*. 2018;18:1-9.
3. Aljamali NM, Al-zubaidy ZH, Enad AH. Bacterial infection and common bacterial diseases: A Review. *Pharm Nanotechnol*. 2021;3:13-23.
4. Matinong AME, Chisti Y, Pickering KL, Haverkamp RG. Collagen extraction from animal skin. *Biology (Basel)*. 2022;11(6):905.
5. Hou NT, Chen BH. Extraction, purification and characterization of collagen peptide prepared from skin hydrolysate of sturgeon fish. *Food Qual Saf*. 2023;7:fyad033.
6. Oslan SNH, Li CX, Shapawi R, Mokhtar RAM, Noordin WNM, Huda N. Extraction and characterization of bioactive fish by-product collagen as promising for potential wound healing agent in pharmaceutical applications: current trend and future perspective. *Int J Food Sci*. 2022;2022(1):9437878.
7. Lo S, Fauzi MB. Current update of collagen nanomaterials—fabrication, characterisation and its applications: a review. *Pharmaceutics*. 2021;13(3):316.
8. Liang W, Zhou C, Bai J, et al. Current developments and future perspectives of nanotechnology in orthopedic implants: an updated review. *Front Bioeng Biotechnol*. 2024;12:1342340.
9. Wosicka-Fraćkowiak H, Poniedziałek K, Woźny S, et al. Collagen and its derivatives serving biomedical purposes: a review. *Polymers (Basel)*. 2024;16(18):2668.

10. Jafari H, Lista A, Siekapen MM, et al. Fish collagen: Extraction, characterization, and applications for biomaterials engineering. *Polymers (Basel)*. 2020;12(10):2230.
11. Lo S, Mahmoudi E, Qi Hao L, Mohd Nor F, Fauzi MB. Fabrication of nanocollagen using enhanced cryogenic milling method with graphene oxide. *Int J Nanomedicine*. 2024;6845-6855.
12. Saod WM, Alaallah NJ, Abdulkareem EA, Hilal NN, AlBiajawi MI. Study of effective removal of nickel and cobalt from aqueous solutions by FeO@mSiO<sub>2</sub> nanocomposite. *Results Chem*. 2025;13:101992.
13. Abd Alkareem E, Abd Al-karim NF, Mahmoud II. Synthesis of New Azo Compounds and Their Application for a Simple Spectrophotometric Determination of Methyldopa Drug Using Anthranilic Acid and 2-Aminopyrimidine as Reagents. *J Turkish Chem Soc Sect A Chem*. 2023;10(3):621-632.
14. De Santis S, Porcelli F, Sotgiu G, et al. Identification of remodeled collagen fibers in tumor stroma by FTIR Micro-spectroscopy: A new approach to recognize the colon carcinoma. *Biochim Biophys Acta (BBA)-Molecular Basis Dis*. 2022;1868(1):166279.
15. Alaallah NJ, Abd Alkareem E, Ghaidan A, Imran NA. Eco-friendly approach for silver nanoparticles synthesis from lemon extract and their anti-oxidant, anti-bacterial, and anti-cancer activities. *J Turkish Chem Soc Sect A Chem*. 2023;10(1):205-216.
16. Elshikh M, Ahmed S, Funston S, et al. Resazurin-based 96-well plate microdilution method for the determination of minimum inhibitory concentration of biosurfactants. *Biotechnol Lett*. 2016;38:1015-1019.
17. Roată CE, Iacob Ștefan, Morărașu Ștefan, et al. Collagen-binding nanoparticles: a scoping review of methods and outcomes. *Crystals*. 2021;11(11):1396.
18. Kahdestani SA, Shahriari MH, Abdouss M. Synthesis and characterization of chitosan nanoparticles containing teicoplanin using sol-gel. *Polym Bull*. 2021;78(2):1133-1148.
19. Kaiser E, Jaganathan SK, Supriyanto E, Ayyar M. Fabrication and characterization of chitosan nanoparticles and collagen-loaded polyurethane nanocomposite membrane coated with heparin for atrial septal defect (ASD) closure. *3 Biotech*. 2017;7:1-12.
20. Alagha A, Nourallah A, Hariri S. Characterization of dexamethasone loaded collagen-chitosan sponge and in vitro release study. *J Drug Deliv Sci Technol*. 2020;55:101449.
21. Swethavinayagam KE, Venkatesan D, Rebecca LJ. Preparation of chitosan nanoparticles and its synergistic effects against gram positive and gram-negative microorganisms. *J Pure Appl Microbiol*. 2019;13(4):2317-2324.
22. Kadhum WN, Zaidan IA. The synergistic effects of chitosan-alginate nanoparticles loaded with doxycycline antibiotic against multidrug resistant proteus mirabilis, Escherichia coli and enterococcus faecalis. *Iraqi J Sci*. 2020;61(12):3187-3319.
23. Al-Ghamdi M, Aly MM, Sheshtawi RM. Antimicrobial activities of different novel chitosan-collagen nanocomposite films against some bacterial pathogens. *Int J Pharm Phytopharm Res*. 2020;10(1):114-121.